

## Piezoelectric response and origin in (001) Pb ( Mg 1 / 3 Nb 2 / 3 ) 0.70 Ti 0.30 O 3 crystal

C.-S. Tu, C.-M. Hsieh, V. Hugo Schmidt, R. R. Chien, and H. Luo

Citation: [Applied Physics Letters](#) **93**, 172905 (2008); doi: 10.1063/1.3012384

View online: <http://dx.doi.org/10.1063/1.3012384>

View Table of Contents: <http://scitation.aip.org/content/aip/journal/apl/93/17?ver=pdfcov>

Published by the [AIP Publishing](#)

---

### Articles you may be interested in

High magnetic field sensitivity in Pb ( Zr , Ti ) O 3 – Pb ( Mg 1 / 3 Nb 2 / 3 ) O 3 single crystal/Terfenol-D/Metglas magnetoelectric laminate composites

J. Appl. Phys. **107**, 094109 (2010); 10.1063/1.3406142

Rapid piezoelectric response and origin in (001) Pb ( In 1 / 2 Nb 1 / 2 ) 0.70 Ti 0.30 O 3 crystal

J. Appl. Phys. **106**, 016102 (2009); 10.1063/1.3157926

Response of polar nanoregions in 68 % Pb ( Mg 1/3 Nb 2/3 ) O 3 - 32 % Pb Ti O 3 to a [001] electric field

Appl. Phys. Lett. **93**, 082901 (2008); 10.1063/1.2959077

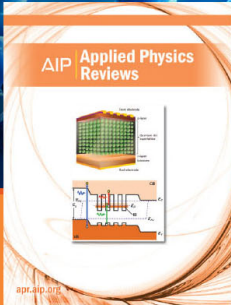
Nanotwins and phases in high-strain Pb ( Mg 1 / 3 Nb 2 / 3 ) 1 – x Ti x O 3 crystal

J. Appl. Phys. **103**, 074117 (2008); 10.1063/1.2904900

Domain-engineered Pb ( Mg 1/3 Nb 2/3 ) O 3 – PbTiO 3 crystals: Enhanced piezoelectricity and optimal domain configurations

Appl. Phys. Lett. **84**, 3930 (2004); 10.1063/1.1745114

---



**NEW Special Topic Sections**

**NOW ONLINE**  
Lithium Niobate Properties and Applications:  
Reviews of Emerging Trends

**AIP** | Applied Physics  
Reviews

## Piezoelectric response and origin in (001) $\text{Pb}(\text{Mg}_{1/3}\text{Nb}_{2/3})_{0.70}\text{Ti}_{0.30}\text{O}_3$ crystal

C.-S. Tu,<sup>1,a)</sup> C.-M. Hsieh,<sup>1</sup> V. Hugo Schmidt,<sup>2</sup> R. R. Chien,<sup>2</sup> and H. Luo<sup>3</sup>

<sup>1</sup>Department of Physics, Fu Jen Catholic University, Taipei 242, Taiwan

<sup>2</sup>Department of Physics, Montana State University, Bozeman, Montana 59717, USA

<sup>3</sup>Shanghai Institute of Ceramics, Chinese Academy of Sciences, Shanghai 201800, People's Republic of China

(Received 28 August 2008; accepted 10 October 2008; published online 30 October 2008)

Converse and direct piezoelectric coefficients ( $d_{33}^C$  and  $d_{33}^D$ ) of (001)-cut  $\text{Pb}(\text{Mg}_{1/3}\text{Nb}_{2/3})_{0.70}\text{Ti}_{0.30}\text{O}_3$  (PMN-30%PT) single crystals have been investigated as a function of poling electric ( $E$ ) field.  $E$ -field-dependent domain structures were observed by using a polarizing microscope. Both  $d_{33}^C$  and  $d_{33}^D$  exhibit a rapid increase at  $E=1-2$  kV/cm and reach maxima at  $E=2.5-4$  kV/cm. This study suggests that polarization rotation from rhombohedral to monoclinic  $M_A$  phases plays an important role while the high piezoelectric response builds up. Overpoling phenomenon evidenced by a sudden reduction in piezoelectric coefficient with increasing field is very sensitive to Ti content.

© 2008 American Institute of Physics. [DOI: 10.1063/1.3012384]

The most attractive feature of relaxor-based ferroelectrics  $\text{Pb}(\text{Mg}_{1/3}\text{Nb}_{2/3})_{1-x}\text{Ti}_x\text{O}_3$  (PMN-PT) is that they have high piezoelectric coefficients compared with lead zirconic titanate ceramics.<sup>1</sup> Ferroelectric (FE) and piezoelectric properties of PMN-PT are sensitive to Ti content, poling  $E$  field, and crystallographic orientation.<sup>1</sup> The ultrahigh piezoelectric response (piezoresponse) has been theoretically attributed to polarization rotations between rhombohedral ( $R$ ) and tetragonal ( $T$ ) phases through monoclinic ( $M$ ) or orthorhombic ( $O$ ) symmetries.<sup>2</sup>

From  $E$ -field-dependent domain observation, a polarization rotation via an  $R-M_A-T_{001}$  transition sequence was evidenced in a (001) PMN-24%PT crystal.<sup>3</sup> Randomly distributed [001]  $T$  domains were observed under  $E=38$  kV/cm in a (001) PMN-30%PT crystal<sup>4</sup> and suggested that the domain matrix consists of dipole glass and FE nanoclusters as proposed for PMN.<sup>5</sup> From synchrotron x-ray diffraction (XRD), an  $M_A$  phase was observed in a (001) PMN-35%PT crystal after poling at  $E=43$  kV/cm, but if only weakly poled the sample exhibits an average  $R$  symmetry.<sup>6</sup> An overpoling was observed in piezoelectric coefficients of flux-grown PMN-(31–32)%PT crystals.<sup>7</sup> No overpoling was seen in PMN-28%PT and PMN-30%PT crystals.<sup>7</sup> A recent  $E$ -field-dependent  $d_{33}$  measurement in a (001) PMN-30%PT crystal showed a dramatic overpoling for  $E \geq 2$  kV/cm due to the appearance of  $M_C$  phase.<sup>8</sup>

The equality of “direct piezoelectric effect ( $P_i=d_{ij}X_j$ )” (the production of surface charge when an external stress is applied) and “converse piezoelectric effect ( $S_j=d_{ij}E_i$ )” (the production of strain when an external  $E$  field is applied) is self-evident.<sup>9</sup> In other words, the piezoelectric coefficient  $d_{ij}=(P_i/X_j)_E=(S_j/E_i)_T$  can be obtained by measuring surface charge density or strain under external stress or  $E$  field, respectively. Here  $P$ ,  $E$ ,  $X$ , and  $S$  represent charge density ( $\text{C}/\text{m}^2$ ),  $E$  field ( $\text{V}/\text{m}$ ), mechanical stress ( $\text{N}/\text{m}^2$ ), and strain, respectively.

In this crystal and other relaxor FE crystals,<sup>7,8</sup> the piezoelectric coefficient often shows a rapid increase with field in

the low-field region, followed by a reduction due to overpoling. No one had explained before with experimental evidence of this rapid piezoresponse increase with  $E$  field in PMN-PT crystals, which is crucial for applications. In this report, we propose that  $R-M_A$  polarization rotation is responsible for this high piezoresponse in the (001) PMN-30%PT crystal. No significant overpoling was observed with increasing field. However, a moderate overpoling was observed in a crystal with a slightly smaller Ti content.

The PMN-30%PT crystal was grown using a modified Bridgman method. The sample was cut perpendicular to a  $\langle 001 \rangle$  direction. The Ti content ( $x$ ) was determined by using the zero-field-heated<sup>4</sup> dielectric maximum temperature  $T_m=414.75$  K at  $f=10$  kHz, i.e.,  $x=[T_m(^{\circ}\text{C})+10](\%)/5 \cong 30.4\%$ .<sup>10</sup> For measurement of the converse piezoelectric coefficient ( $d_{33}^C$ ), a Rigaku Model MultiFlex x-ray diffractometer with  $\text{Cu } K\alpha_1$  and  $\text{Cu } K\alpha_2$  radiations was used for determination of  $d$  spacing. The widths of divergence and scattering slits are  $0.5^{\circ}$  and the cross section of the x-ray beam on the sample is greater than  $4 \times 4$  mm<sup>2</sup>. The sample dimensions are  $5.7 \times 4.0 \times 0.6$  mm<sup>3</sup> and the basal surfaces were coated with thin gold electrodes (thickness  $\cong 30$  nm). The intensity ratio of  $K\alpha_1$  and  $K\alpha_2$  radiations is about 2:1.<sup>11</sup> The conventional x-ray penetration depth is less than 10  $\mu\text{m}$ .<sup>12</sup> The XRD spectra were fitted with a sum of Gaussian and Lorentzian terms.

Two processes were used in the XRD scans. The first is called “prior poled before zero-field” (PP-ZF), in which the crystal was poled along [001] by a dc voltage at room temperature for 20 min and then the XRD scan was performed without  $E$  field. In the “nonzero-field” (NZF) process, the crystal was poled at room temperature for 20 min and then the XRD scan was performed under the same  $E$  field. The  $E$  field was raised in steps in both PP-ZF and NZF. Hereafter,  $d_{E=0}$  and  $d_{E \neq 0}$  represent the  $d$  spacings obtained from the first and second processes, respectively. The  $2\theta$  reflection and  $d$  spacing obey the Bragg law  $2d \sin \theta = n\lambda$ . The strain ( $S_3$ ) and  $d_{33}^C$  were calculated by the equations,  $S_3(\%) = (d_{E \neq 0} - d_{E=0}) \times 100\% / d_{E=0}$  and  $d_{33}^C = E_3 / S_3$ .

The direct (or normal) piezoelectric coefficient ( $d_{33}^D$ ) was measured by using a model ZJ-6B quasistatic piezo- $d_{33}/d_{31}$

<sup>a)</sup>Author to whom correspondence should be addressed. Electronic mail: 039611@mail.fju.edu.tw.

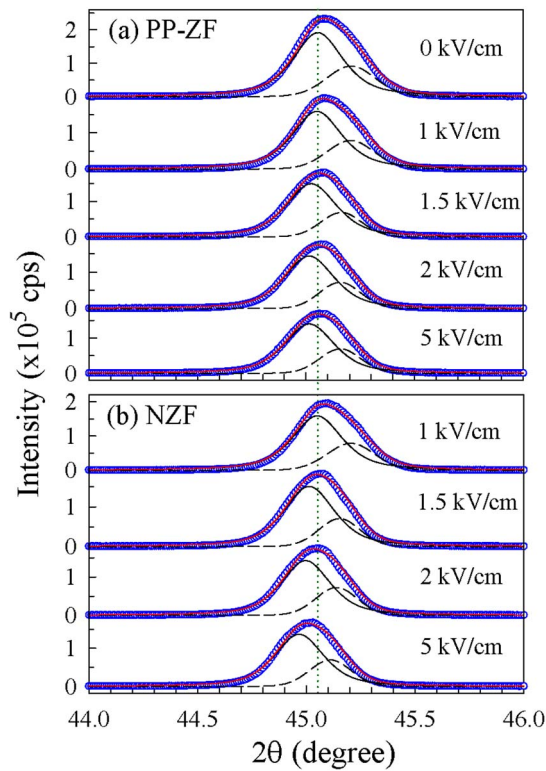


FIG. 1. (Color online)  $E$ -field-dependent (002) (a) PP-ZF and (b) NZF XRD spectra. The solid and dashed lines correlate to the  $K\alpha_1$  and  $K\alpha_2$  radiations, respectively. The red solid line is the sum of fittings. The dotted line is a guide for the XRD shifts.

meter.  $d_{33}^D$  was obtained by measuring the surface charge density ( $P$ ) under a stress along [001], i.e.,  $d_{33}^D = P_3/X_3$ . Before each  $d_{33}^D$  measurement, the sample was poled along [001] by a dc voltage at room temperature for 20 min.

$E$ -field-dependent domain structures were observed by using a Nikon E600POL polarizing microscope with a crossed polarizer/analyzer (P/A) pair. Transparent conductive films of indium tin oxide were deposited on the (001) surfaces. The sample thickness is about 70  $\mu\text{m}$ . Angles of the P/A pair measured are with regard to the [110] direction. The experiment and details for using optical extinction to determine domain phases can be found in Refs. 1 and 3.

Figure 1(a) shows the (002) PP-ZF XRD spectra at different poling  $E$  fields. The XRD peak shows a shift toward low- $2\theta$  positions as  $E$  field increases. A significant shift occurs at  $E=1-2$  kV/cm, which is slightly less than the coercive field of  $E_C \cong 2.2$  kV/cm measured at 46 Hz.<sup>4</sup> Above  $E=2.0$  kV/cm, the XRD position exhibits a rather gradual change as  $E$  field increases. Similar  $E$ -field-dependent behavior was observed in the (002) NZF XRD spectra as seen in Fig. 1(b), which shows a rather significant shift at  $E=1-2$  kV/cm.

By using the Bragg law from the  $K\alpha_1$  radiation, both  $d$  spacing and full width at half maxima ( $\delta_{\text{FWHM}}$ ) are plotted in Fig. 2 as a function of  $E$  field. The accuracy of  $d$  spacing is better than 0.1%. Both  $d$  spacing and  $\delta_{\text{FWHM}}$  exhibit a significant response at  $E=1-2$  kV/cm, especially for the NZF XRD spectra.  $d_{E \neq 0}$  and  $d_{E=0}$  spacings exhibit an approximately linear response at  $E \geq 2.0$  kV/cm. A small but obvious reduction in  $\delta_{\text{FWHM}}$  that occurs at  $E \geq 2.0$  kV/cm in both PP-ZF and NZF XRD spectra suggests a sudden in-

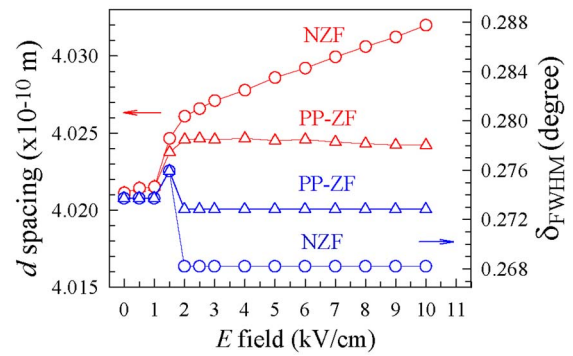


FIG. 2. (Color online)  $E$ -field-dependent  $d$  spacing and  $\delta_{\text{FWHM}}$ .

crease in domain size, especially in the NZF.

Figure 3 shows  $E$ -field-dependent  $d_{33}^C$  and  $d_{33}^D$ . Both  $d_{33}^C$  and  $d_{33}^D$  exhibit a rapid and large growth at  $E=1-2$  kV/cm and reach maxima of about 2100 and 1600 pC/N, respectively. The  $d_{33}^D$  is the average value measured from positions near the center of the sample. An obvious variation of about 50% in  $d_{33}^D$  was observed at different positions on the sample surface. A significant variation ( $>80\%$ ) in  $d_{33}^D$  was reported in a (001) PMN-30%PT crystal.<sup>8</sup> The reason why  $d_{33}^C$  is about 30% larger than  $d_{33}^D$  at  $E \geq 3$  kV/cm is possibly a spatial variation in Ti content. In addition, surface current leakage may occur in the  $d_{33}^D$  measurement and causes a reduction below the true value.

To understand what causes the rapid piezoresponse at  $E=1-2$  kV/cm,  $E$ -field-dependent domain structures were observed as given in Fig. 4. Most of the domain matrix at zero field has an extinction angle at  $P/A=0^\circ$ , indicating that the major phase is rhombohedral. There is no obvious change in the extinction angle at  $E=0-2$  kV/cm in which the piezoelectric coefficient increases rapidly.

To explain the above results, we examine their consistency with three hypotheses. The first hypothesis is that the field induces a  $T$  domain polarized along [001]. This would require that the extinction angle changes from  $0^\circ$  to  $45^\circ$ , which does not occur. The second hypothesis is that the field applied along [001] favors the four  $R$  domains with a polarization component along [001]. Field-induced rotation of

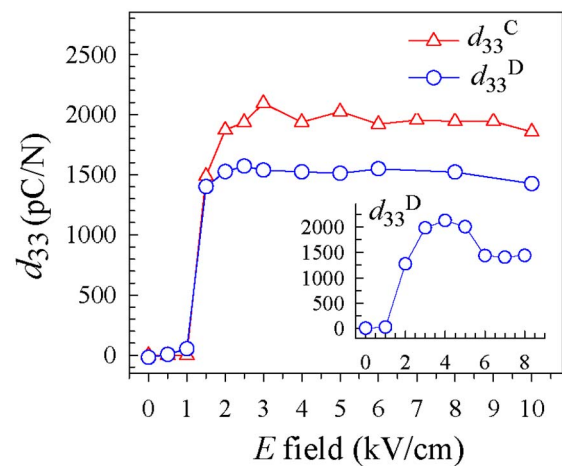


FIG. 3. (Color online)  $E$ -field-dependent piezoelectric coefficients  $d_{33}^D$  (circle symbol) and  $d_{33}^C$  (triangle symbol). The inset is the maximum  $d_{33}^D$  obtained from another (001) PMN-30%PT crystal with 29.6% Ti content.

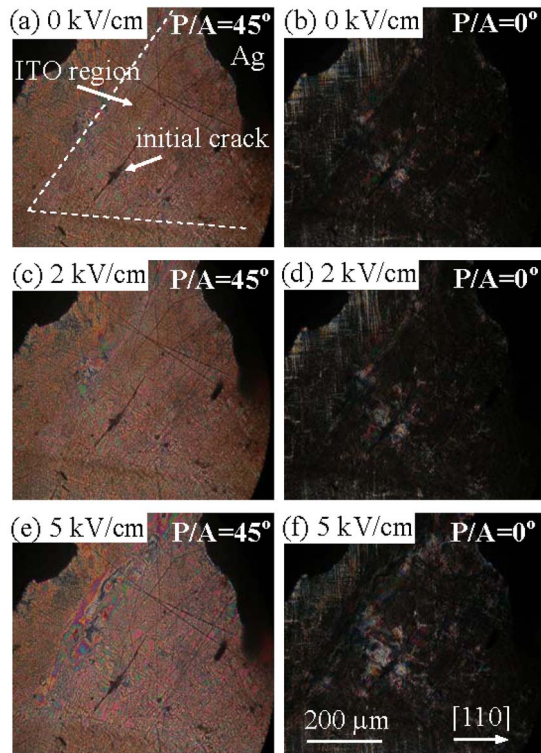


FIG. 4. (Color online)  $E$ -field-dependent domain structures observed at  $P/A=45^\circ$  and  $0^\circ$ .

these vectors and the accompanying structure has been thought according to the principles of “domain engineering” to account for the large  $d_{33}$  once the field has succeeded in reducing the number of domain types from eight to four. The major drawback of this hypothesis is that the PP-ZF XRD result in Fig. 2 shows  $d$  spacing increasing with field from 4.021 to about 4.025 Å. Conversion of an antialigned domain such as  $[\bar{1}, \bar{1}, \bar{1}]$  to its aligned  $[1, 1, 1]$  opposite polarization direction does not require any change in the unit cell shape or orientation; only the internal ionic configuration changes. Accordingly, there should be no change in  $d$  once the field is removed in the PP-ZF. The third hypothesis is that the field, perhaps after reducing the number of domain types from eight to four, changes these  $4R$  domain types to the  $4M_A$  domain types with similar polarization directions.

According to the optical extinction principles for the (001) orientation,<sup>3</sup> these  $M_A$  domain types have the same  $0^\circ$  extinction angle as the  $R$  phase. As shown in Figs. 1 and 2, the XRD peak exhibits a dramatic shift at  $E=1-2$  kV/cm and remains at the same shifted value for larger fields in the PP-ZF experiment. If the shift was caused by field-induced strain that does not completely relax when the field is removed, one would expect  $d$  to increase with  $E$  for  $E > 2$  kV/cm. On the contrary, this independence of shift from prior  $E$  magnitude is consistent with the third hypothesis because once the field is large enough to induce the  $M_A$  phase, for PP-ZF the  $d$  spacing stays at the equilibrium value

for that phase and is not affected by how large the field was. These results suggest that the dramatic piezoresponse at  $E=1-2$  kV/cm is caused by polarization rotation from  $R$  to  $M_A$  phases. This is consistent with the first-principles calculation of  $\text{BaTiO}_3$ ,<sup>2</sup> which predicts that the minimum energy path (with a rapid increase in strain) of polarization rotation from  $\langle 111 \rangle$  to  $\langle 001 \rangle$  is the  $M_A$  phase. At  $E > 2$  kV/cm as shown in Figs. 4(e) and 4(f), more domains have extinctions at  $P/A \neq 0^\circ$ , implying a gradual expansion of  $M$  phase (possible  $M_A$ ) in the matrix.<sup>4</sup> Of the 24 types of  $M_A$  domains, only eight have extinction angle at  $0^\circ$ .

The inset in Fig. 3 shows the  $d_{33}^D$  (which is the maximum value) obtained from another (001) PMN-30%PT crystal whose zero-field-heated dielectric maximum temperature is  $T_m=410.81$  K at  $f=10$  kHz, i.e.,  $x \cong 29.6\%$ . The  $d_{33}^D$  reaches a maximum of about 2100 pC/N near  $E=4$  kV/cm and then a moderate overpoling appears at  $E \geq 6$  kV/cm. A dramatic overpoling was reported in a (001) PMN-30%PT and was attributed to the  $M_C$  phase.<sup>8</sup> The main reason to cause the diversity among (001) PMN-30%PT crystals seen in Fig. 3 and Ref. 8 is composition segregation, especially for  $x \cong 30\%$  which locates at the morphotropic phase boundary.<sup>13</sup>

In conclusion, the (001) PMN-30%PT crystal exhibits a rapid increase in both  $d_{33}^C$  and  $d_{33}^D$  at  $E=1-2$  kV/cm. The origin of this rapid increase in piezoresponse is polarization rotation through the  $R-M_A$  transformation. This study suggests that polarization rotation, which is consistent with first-principles calculations,<sup>2</sup> plays a crucial role in providing the high piezoresponse. No significant overpoling was observed in the (001) PMN-30.4%PT crystal. However, a moderate overpoling was observed in the crystal with 29.6% Ti content.

This work was supported by National Science Council of Taiwan Grant under Contract No. 96-2112-M-030-001.

<sup>1</sup>P. Han *et al.*, *Handbook of Advanced Dielectric, Piezoelectric and Ferroelectric Materials*, edited by Z.-G. Ye (Woodhead, Cambridge, 2008).

<sup>2</sup>H. Fu and R. E. Cohen, *Nature (London)* **403**, 281 (2000).

<sup>3</sup>R. R. Chien, V. H. Schmidt, C.-S. Tu, L.-W. Hung, and H. Luo, *Phys. Rev. B* **69**, 172101 (2004).

<sup>4</sup>C.-S. Tu, C.-M. Hsieh, R. R. Chien, V. H. Schmidt, F.-T. Wang, and W. S. Chang, *J. Appl. Phys.* **103**, 074117 (2008).

<sup>5</sup>R. Blinc, V. V. Laguta, and B. Zalar, *Phys. Rev. Lett.* **91**, 247601 (2003).

<sup>6</sup>Z.-G. Ye, B. Noheda, M. Dong, D. Cox, and G. Shirane, *Phys. Rev. B* **64**, 184114 (2001).

<sup>7</sup>M. Shanthi, K. H. Hoe, C. Y. H. Lim, and L. C. Lim, *Appl. Phys. Lett.* **86**, 262908 (2005).

<sup>8</sup>A. A. Bokov and Z.-G. Ye, *Appl. Phys. Lett.* **92**, 082901 (2008).

<sup>9</sup>T. Ikeda, *Fundamentals of Piezoelectricity* (Oxford University Press, New York, 1990).

<sup>10</sup>Z. Feng, H. Luo, Y. Guo, T. He, and H. Xu, *Solid State Commun.* **126**, 347 (2003).

<sup>11</sup>B. D. Cullity, *Elements of X-Ray Diffraction*, 2nd ed. (Addison-Wesley, Reading, MA, 1978), pp. 8–10.

<sup>12</sup>G. Xu, H. Hiraka, G. Shirane, and K. Ohwada, *Appl. Phys. Lett.* **84**, 3975 (2004).

<sup>13</sup>B. Noheda, D. E. Cox, G. Shirane, J. Gao, and Z.-G. Ye, *Phys. Rev. B* **66**, 054104 (2002).